Ecological Applications, 0(0), 2019, e01952

Persistent effects of fragmentation on tropical rainforest canopy structure after 20 yr of isolation

Danilo R. A. Almeida,[1,15] Scott C. Stark,[2] Juliana Schietti,[3] Jose L. C. Camargo,[4] Nino T. Amazonas,[1] Eric B. Gorgens,[5] Diogo M. Rosa,[3] Marielle N. Smith,[2] Ruben Valbuena,[6,7] Scott Saleska,[8] Ana Andrade,[4] Rita Mesquita,[3,4] Susan G. Laurance,[9] William F. Laurance,[8] Thomas E. Lovejoy,[4] Eben N. Broadbent,[10] Yosio E. Shimabukuro,[11] Geoffrey G. Parker,[12] Michael Lefsky,[13] Carlos A. Silva,[14] and Pedro H. S. Brancalion[1]

[1]*Department of Forest Sciences, "Luiz de Queiroz" College of Agriculture, University of São Paulo (USP/ESALQ), Avenida Pádua Dias, 11, Piracicaba, São Paulo 13418-900 Brazil*
[2]*Department of Forestry, Michigan State University, East Lansing, Michigan 48824 USA*
[3]*National Institute for Amazonian Research (INPA), Avenida André Araújo, Manaus, Amazonas 2936, 69067-375 Brazil*
[4]*Biological Dynamics of Forest Fragments Project (BDFFP), National Institute for Amazonian Research (INPA) and Smithsonian Tropical Research Institute, Manaus 69067-375 Brazil*
[5]*Department of Forestry, Federal University of Vales do Jequitinhonha e Mucuri, Campus JK, Rodovia MGT 367 - Km 583, n° 5000, Diamantina, Brazil*
[6]*Department of Plant Sciences, Forest Ecology and Conservation, University of Cambridge, Downing Street, Cambridge CB2 3EA United Kingdom*
[7]*School of Natural Sciences, Bangor University, Bangor LL57 2UW United Kingdom*
[8]*Department of Ecology and Evolutionary Biology, University of Arizona, 1041 E. Lowell Street, Tucson, Arizona 85721 USA*
[9]*College of Science and Engineering, Centre for Tropical Environmental and Sustainability Science, James Cook University, Cairns, Queensland 4878 Australia*
[10]*School of Forest Ecology and Conservation, Spatial Ecology and Conservation Lab, University of Florida, 303 Reed Lab, Gainesville, Florida 32611 USA*
[11]*National Institute for Space Research (INPE), Avenida dos Astronautas, São Jose dos Campos, São Paulo 1758, 12201 Brazil*
[12]*Smithsonian Environmental Research Center, 647 Contee's Wharf Road, Edgewater, Maryland 21037 USA*
[13]*Department of Ecosystem Science and Sustainability, Colorado State University, Fort Collins, Colorado 80523-1476 USA*
[14]*Biosciences Laboratory, NASA Goddard Space Flight Center, Greenbelt, Maryland 20707 USA*

Citation: Almeida, D. R. A., S. C. Stark, J. Schietti, J. L. C. Camargo, N. T. Amazonas, E. B. Gorgens, D. M. Rosa, M. N. Smith, R. Valbuena, S. Saleska, A. Andrade, R. Mesquita, S. G. Laurance, W. F. Laurance, T. E. Lovejoy, E. N. Broadbent, Y. E. Shimabukuro, G. G. Parker, M. Lefsky, C. A. Silva, and P. H. S. Brancalion. 2019. Persistent effects of fragmentation on tropical rainforest canopy structure after 20 yr of isolation. Ecological Applications 00(00): e01952. 10.1002/eap.1952

Abstract. Assessing the persistent impacts of fragmentation on aboveground structure of tropical forests is essential to understanding the consequences of land use change for carbon storage and other ecosystem functions. We investigated the influence of edge distance and fragment size on canopy structure, aboveground woody biomass (AGB), and AGB turnover in the Biological Dynamics of Forest Fragments Project (BDFFP) in central Amazon, Brazil, after 22+ yr of fragment isolation, by combining canopy variables collected with portable canopy profiling lidar and airborne laser scanning surveys with long-term forest inventories. Forest height decreased by 30% at edges of large fragments (>10 ha) and interiors of small fragments (<3 ha). In larger fragments, canopy height was reduced up to 40 m from edges. Leaf area density profiles differed near edges: the density of understory vegetation was higher and midstory vegetation lower, consistent with canopy reorganization via increased regeneration of pioneers following post-fragmentation mortality of large trees. However, canopy openness and leaf area index remained similar to control plots throughout fragments, while canopy spatial heterogeneity was generally lower at edges. AGB stocks and fluxes were positively related to canopy height and negatively related to spatial heterogeneity. Other forest structure variables typically used to assess the ecological impacts of fragmentation (basal area, density of individuals, and density of pioneer trees) were also related to lidar-derived canopy surface variables. Canopy reorganization through the replacement of edge-sensitive species by disturbance-tolerant ones may have mitigated the biomass loss effects due to fragmentation observed in the earlier years of BDFFP. Lidar technology offered novel insights and observational scales for analysis of the

Manuscript received 30 January 2019; accepted 23 April 2019. Corresponding Editor: Michael Keller.
[15] E-mail: daniloflorestas@gmail.com

ecological impacts of fragmentation on forest structure and function, specifically aboveground biomass storage.

Key words: airborne laser scanner; Amazon; biological dynamics of forest fragments project; edge effects; forest degradation; forest dynamics; forest succession; land use change; leaf area density; lidar; vegetation structure.

Introduction

The effects of forest fragmentation on biodiversity, structure, and function of tropical forest remnants are an important issue in conservation biology due to its close association with land use change (Ewers et al. 2011, Laurance et al. 2017). Globally, it is estimated that there are more than 50 million tropical forest fragments, comprising an area of almost 300 million hectares, with 50 million linear kilometers of edges (Brinck et al. 2017). The air near forest edges is drier and hotter, light incidence is higher, and winds are stronger (Kapos 1989, Camargo and Kapos 1995, Didham and Lawton 1999). Such alterations in forest microclimate have favored the replacement of large late-successional trees by light-wooded, fast-growing pioneers (Bierregaard et al. 1992, Ferreira and Laurance 1997), and are one of the major drivers of forest biomass collapse near edges (Laurance et al. 1997, 2000) and net carbon emissions after fragmentation (Brinck et al. 2017). The consequences of fragmentation for tropical forest structure and function are thus critical for understanding global changes in biodiversity and climate (Laurance et al. 1998, Broadbent et al. 2008, Chaplin-Kramer et al. 2015). Prior assessments of the ecological impacts of tropical forest fragmentation, however, have primarily been short-term studies focusing on forest plot inventories, which limits scales of inference, knowledge about canopy structure and function changes, and, broadly, understanding of the persistent impacts and global relevance of fragmentation.

The scarce quantitative information available on the impacts of fragmentation on the canopy structure of tropical forests was gathered through time consuming, local-scale visual methods with limited accuracy and precision (Camargo and Kapos 1995, Didham and Lawton 1999). The findings of these previous studies have mostly shown that forest fragmentation increases the frequency of gaps and reduces canopy height due to high initial mortality of large remnant trees (Kapos 1989, Ferreira and Laurance 1997, Laurance et al. 1998, 2006*a*, D'Angelo et al. 2004, Nascimento and Laurance 2006). For instance, Camargo and Kapos (1995) found that the density of understory trees (<5 m height) was higher, and density of midstory trees (10–30 m height) was lower, in 4-yr-old fragment edges compared to the forest interior and adjacent non-fragmented forests in the central Amazon of Brazil. Didham and Lawton (1999) found that these structural effects persisted ten years after fragmentation in the same experiment. However, it is not yet clear if the aboveground biomass (AGB) decline observed in the first years of fragmentation persists over time, since initial AGB loss from remnant tree mortality can gradually recover from the regeneration of new trees in the community (Laurance et al. 2017).

Technological advances in remote sensing now allow for high precision, fast, and broad-scale quantitative three-dimensional characterization of forest canopy structure (Lefsky et al. 2002, Chambers et al. 2007). Lidar, or light detection and ranging, technology provides unique quantitative information about forest canopy structure, including vertical and horizontal variation in the density of vegetation surfaces, allowing for linkage of forest structure to forest function (Lefsky et al. 2002, Tang and Dubayah 2017, Valbuena et al. 2017). The application of lidar technology to tropical forests is rapidly expanding and has been used to estimate canopy height, openness and spatial heterogeneity (coefficient of variation in canopy heights), leaf area index (LAI), and vegetation density profiles, which can be linked to AGB and AGB dynamics (van Leeuwen and Nieuwenhuis 2010, Stark et al. 2012, Simonson et al. 2014, de Almeida et al. 2016). The Biological Dynamics of Forest Fragments Project (BDFFP) in the Central Brazilian Amazon is one of the largest and oldest (>30 yr) controlled experiments on forest fragmentation and has contributed fundamentally to our understanding of the consequences of fragmentation for forest diversity, dynamics, and function (Lovejoy et al. 1984, Ewers et al. 2011, Laurance et al. 2017). The use of lidar technology to evaluate fragmentation impacts on forest AGB and canopy structure in this experiment offers the opportunity to complement previous studies performed with traditional methods and provide new insights about the longer-term impacts of fragmentation.

Here, we investigated the persistent impacts of edge effects and fragment size on canopy structure and AGB at the BDFFP in fragments that were more than 20 yr old (with original boundaries continuously maintained) at the time of sampling. We associated canopy metrics generated from portable canopy profiling lidar (PCL) surveys conducted in 2015, and airborne laser scanning (ALS) surveys conducted in 2008, with forest inventory data from 2008–2009. We extend the previously reported AGB and forest dynamics results by 10 yr (Laurance et al. 2006*a* most recently reported on a 1999 re-census). This study has implications for both the ecology of and technology used to monitor forest fragmentation. We addressed the following questions:

1. Is canopy height influenced by proximity to forest edges and fragment size?.—We hypothesized that canopy height will increase with distance from the forest edge,

and that the mean canopy height of small fragments (up to 3 ha) and of the edges of larger fragments will be lower than that of the interior of larger fragments (>10 ha) and continuous forest, as consequence of higher mortality of large remnant trees in forest edges and small fragments.

2. Are canopy openness and spatial heterogeneity influenced by proximity to forest edges and fragment size?.—We hypothesized that the canopy would be more open and have greater spatial heterogeneity (i.e., higher horizontal spatial heterogeneity in terms of the coefficient of variation in canopy surface height) closer to forest edges, especially in smaller fragments, as a consequence of higher mortality of large remnant trees in forest edges.

3. Are LAI and LAD profiles of different vertical strata influenced by proximity to forest edges?.—We hypothesized that leaf area index (LAI) and vertical profiles of leaf area density (LAD) at fragment interiors would be similar to those within continuous forest, but reduced near fragment edges. LAI and LAD of low-stature understory vegetation may be higher near edges due to higher light availability, but reduced in upper strata because of the mortality of large trees.

4. Do negative impacts of edge proximity on basal area, AGB, and density of trees persist more than 20 yr after fragmentation?.—We hypothesized that negative influences of proximity to forest edge on basal area, AGB, and tree density observed primarily in the first five years following fragmentation will persist for more than 20 years after fragmentation. Continued degradation or partial recovery are possible alternatives.

5. Are canopy structure variables obtained by lidar able to reveal field metrics of fragmentation impacts?.—We hypothesized that lidar-derived metrics linked with canopy structure can be used to reliably estimate field metrics, such as of basal area, AGB, density of trees individuals, and density of pioneer trees, which can help reveal the impacts of fragmentation.

Methods

Study area and forest inventories

The study area is located in central Amazon, 80 km north of Manaus, in the state of Amazonas, Brazil (2°30′ S, 60°00′ W; Fig. 1). Vegetation is characterized as dense, "terra-firme" (not seasonally flooded) tropical rainforest, with more than 280 tree species per hectare (De Oliveira and Mori 1999); soils are acidic and nutrient poor, elevation varies from 50–100 m above sea level, and annual precipitation varies from 1,900 to 3,500 mm, with a dry period from June to October (climate type: Af, Köppen classification; Laurance et al. 2017). The study area is surrounded by continuous, non-fragmented forest (>200 km from any forest edges) to the north, east, and west. In the 1980s, 11 fragments with three distinct size classes (~2, ~10, and 100 ha) were isolated at distances between 70 and 1,000 m from a continuous

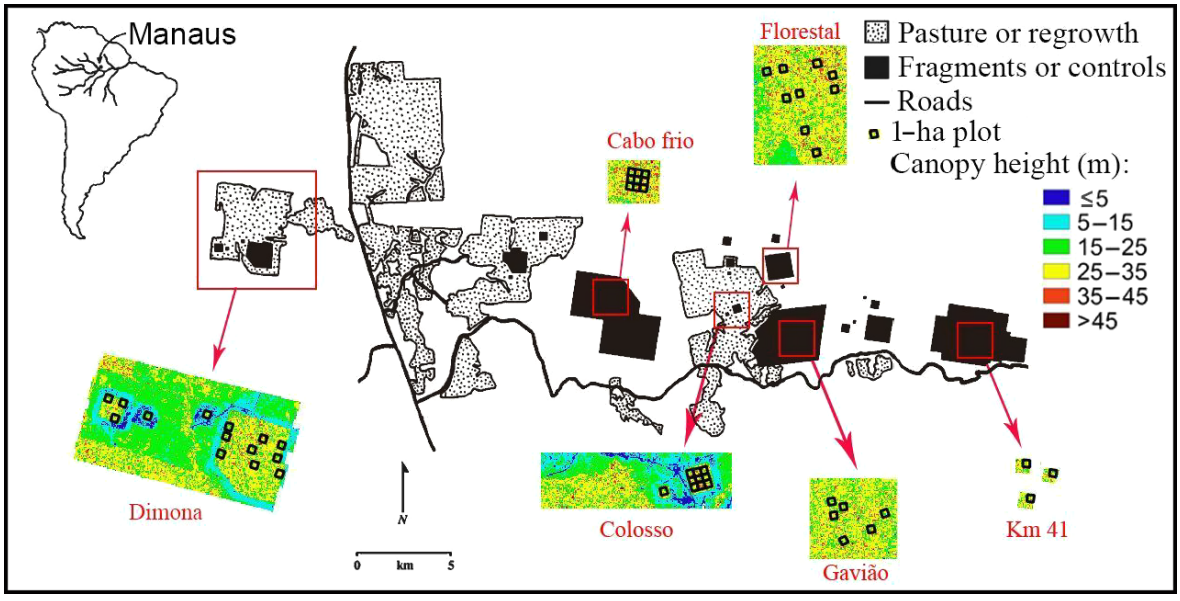

Fig. 1. Location of study sites at the Biological Dynamics of Forest Fragments Project near Manaus, central Amazon, Brazil. The black polygons represent the forest fragments and controls, the dotted areas around them represent pasturelands, and the white background represents continuous forests. Colored figures show the canopy height model, derived by airborne laser scanner, for each experimental site. The black squares within the colored figures are the 1-ha permanent inventory plots used in the study.

forest. Fragments at the Colosso site (Fig. 1) were isolated in July and August 1980 and the surrounding remnant vegetation and debris burned. Thereafter, some of the surrounding areas were maintained as pasture, while others were abandoned to become secondary forest. Secondary forest was recut in 1987 and maintained as pasture thereafter. The fragments at the Dimona site (Fig. 1) were isolated in August and September 1984 and had their surrounding areas burned. The clear-cut area was maintained as pasture thereafter, and original borders are very distinct and have been maintained throughout the study. Fragments were not affected by logging or other disturbance factors once isolated; therefore, turnover and canopy change are purely the result of demographic and ecological processes.

Since the start of the BDFPP experiment, forest inventories have been carried out at 5-yr intervals in 69 1-ha plots distributed within the forest fragments (edges and interiors) and also in control plots in the adjacent continuous forest (Cabo frio, Florestal, Gavião, and Km 41 sites; Fig. 1). This study used data from 51 of the plots, those surveyed with lidar, described in the next section. To date, plots have been inventoried five to eight times. All trees with diameter at breast height (DBH) > 10 cm were identified and recorded. The following variables were calculated with data from each inventory: basal area, tree density, pioneer species density, and AGB, as further described.

Lidar data collection

The airborne laser scanning (ALS) data were collected in June 2008 (>20 yr after fragmentation) by a private company (Esteio Company, Curitiba, PR, Brazil) using a Leica ALS50 system (Heerbrugg, Switzerland) on board a Navajo EMB 820C aircraft (Embraer Company, São José dos Campos, SP, Brazil). The small footprint point cloud was acquired with a return density of 12.2 points/m^2 (~10 pulses/m^2), an average flight height of 725 m, maximum scan angle of 24°, and a ground footprint diameter of 11 cm. Coverage included six forest fragments (three of ~2 ha, two of ~10 ha, and one of 100 ha) and four adjacent continuous forests, totaling 51 plots (3 in ~2-ha fragments, 12 in ~10-ha fragments, 9 in 100-ha fragments, and 27 in continuous forest; Fig. 1).

Profiling lidar (PCL; Parker et al. 2004) data were collected in 18 plots during July 2015 (~30 yr after fragmentation), of which nine were located in the 100-ha fragment (Dimona site) and nine in adjacent continuous forest (Forestal site; Fig. 1). In each plot, two linear transects of 100 m each were established 40 m apart. These transects were parallel to the fragment edge and were considered independent sampling units, each with its respective distance from the edge (Appendix S1: Fig. S1). The PCL system employs a profiling range-finder type laser, model LD90-3100VHS-FLP manufactured by Riegl (Horn, Austria). The PCL accuracy is ±25 mm and the nominal range is 200 m. The equipment records 2,000 pulses per second (Appendix S1: Fig. S2). The instrument is held in a gimbal (1 m above the ground) to maintain vertical aim (Stark et al. 2012, de Almeida et al. 2016). The operator walks at a constant pace along the transect, controlling the speed (0.33 m/s) with the aid of an electronic metronome and markers spaced every 2 m.

Although we used two different lidar technologies, ALS and PCL, both are based on the same principles and produce comparable results (Stark et al. 2012, Almeida et al. 2019).

Lidar data processing

airborne laser scanning and portable canopy profiling lidar pulse reflection point clouds were processed to estimate canopy biophysical properties; data processing was done in R (R Core Team 2017). The ALS cloud was divided into columns of $2 \times 2 \times Z$ m (Z is the highest return within the 2×2 horizontal grid cell). After ensuring that there were no clear outlier return elevations, the digital terrain model (DTM) was created by analyzing the minimum points from each 2×2 cell (raw ground; Appendix S1: Fig. S3). A smooth quantile spline regression from qsreg R function in the fields package (Nychka et al. 2015), was applied to produce the DTM (taken as lowest values of individual lowest 0.05th quantile spline fits to all horizontal columns and rows in the raw ground image; Appendix S1: Fig. S4). This preferred DTM was selected based upon comparison, including visual analysis, against other common alternatives (Appendix S1: Fig. S5). The digital surface model (DSM) was generated using the maximum points of each column (Appendix S1: Fig. S6). The canopy height model (CHM), used to estimate the structural canopy attributes, was calculated as the difference between DSM and DTM (Appendix S1: Fig. S7). Three structural canopy attributes were calculated based on ALS products: (1) the average canopy height (CHM mean), (2) canopy openness (fraction of CHM cells lower than the 15-m-high threshold), and (3) spatial heterogeneity (CHM coefficient of variation; Table 1). According to Runkle (1982), a 15-m cutoff maximizes the sensitivity of this metric to gaps spanning early through middle stages of regeneration.

Airborne laser scanning scenes were classified as open matrix (cleared) or forest (fragment or otherwise) via a manual edge demarcation of CHM rasters using QGIS (QGIS Development Team 2015). Edges were clear and distinct and easy to demarcate with reference to the CHM due to the careful maintenance of the original edges with periodic manual clearing. Distance from the edge was calculated from the median of all linear distances within the plot at a resolution of 2×2 m. We confirmed that distance from the edge did not consistently covary with elevation, slope, or aspect of the terrain.

Each 100-m PCL transect was divided into 50 2-m columns and subdivided into 1-m intervals along the vertical profile (Appendix S1: Fig. S8a). Vertical profiles of

TABLE 1. Data sets used in this study to generate forest structure metrics to evaluate research questions (described at the end of *Introduction*).

Collection data	Method	Metrics obtained	Questions
Collected in 2008	airborne laser scanning (ALS)	canopy height, spatial heterogeneity, and canopy openness	(1), (2) and (5)
Collected in 2015	portable canopy profiling lidar (PCL)	leaf area density (LAD) profiles and leaf area index (LAI) for different vertical strata	(3)
1980–2008, including 2008, which corresponded with the ALS survey year	long-term forest inventory	basal area, aboveground biomass, density of trees, density of pioneer tree species	(4) and (5)

LAD were estimated using the MacArthur and Horn (1969) equation, using the method proposed by de Almeida et al. (2016) (Appendix S1: Fig. S8b). In summary, the method is based on the rates at which ranging pulses pass through (vs. are reflected) within units of canopy volume, providing a basis to estimate volumetric variation in vegetation density from optical transmission rates (MacArthur and Horn 1969, Parker et al. 2004, Stark et al. 2012). Pulses are reflected by leaves, branches, and other structural elements. The PCL approach, however, has been calibrated against independent LAI estimates, including destructive leaf area sampling, for sites in the region with the aim of effectively factoring out the influence of non-leaf area (McWilliam et al. 1993, Stark et al. 2012). LAD profiles were generated by calculating the mean LAD at each height, and LAI was calculated by summing all LAD values in the vertical profile (Almeida et al. 2019).

We established four vertical strata within each LAD profile: understory (1–5 m), the lower-middle (5–15 m), upper-middle (15–25 m), and upper canopy (>25 m). We assessed potential relationships between these strata-specific total LAI values ($LAI_{1–5\ m}$, $LAI_{5–15\ m}$, $LAI_{15–25\ m}$, $LAI_{25–45\ m}$) and distance from edges with regression analysis.

Field data processing

We calculated AGB from tree inventory data applying the Chave et al. (2014) diameter allometry to all non-pioneer trees (Eq. 1), and Nelson et al. (1999) allometry to pioneers (Eq. 2):

$$\mathrm{AGB(kg)} = \exp(-1.803 - 0.976E + 0.976\ln(\mathrm{WD}) + 2.673\ln(\mathrm{DBH}) - 0.0299[\ln(\mathrm{DBH})]^2) \quad (1)$$

$$\mathrm{AGB(kg)} = \exp(-1.4278 + 2.3836\log(\mathrm{DBH}) + 0.7655\log(\mathrm{WD}) \quad (2)$$

where E is a measure of environmental stress (which improves estimation when field measurements of tree height are not available), WD is the wood density, and DBH is the diameter at breast height. The environmental coefficient for the study area ($E = -0.127$) was obtained from the retrieve_raster function (Chave et al. 2014) in R, and the wood density for each tree, based on species, genus, or family identity, according to availability, was obtained from the Global Wood Density Database (Zanne et al. 2009). Wood density estimates were obtained at the species level for 57% of individuals, at the genus level for 39%, at the family level for 3%, and the remaining 1% of trees were assigned the plot average. Because pioneers tend to have lower wood densities and distinct allometric relations, we used the equation for pioneer species of Nelson et al. (1999) to estimate their biomass (Eq. 2). We determined pioneer trees based on a list of 52 species classified as pioneers by Laurance et al. (2006*b*).

Tree inventory data were available for the year of the ALS survey (Table 1). PCL variables (LAD profiles), however, were collected in surveys 7 yr later; thus we did not directly compare these with ALS and field variables.

Data analysis

We related canopy biophysical properties to fragmentation and forest plot variables with statistical model fitting. First, an exponential model (Eq. 3) related canopy height (CH; m) to distance from the edge of a fragment (dist; m):

$$\mathrm{CH} = \alpha + (\beta - \alpha)\exp\left(\frac{-(\mathrm{dist})}{\gamma}\right) \quad (3)$$

where alpha (α) is the asymptote of the model representing the height of the vegetation at the interior of the fragment, beta (β) is the intercept of the model and represents the height of the vegetation at the edge of the fragment, and gamma (γ) is related to the rate of change in canopy height when increasing the distance to the edge of fragment. The model was fit with a nonlinear least squares method. Values of the alpha and beta coefficients of each forest fragment were compared to assess the potential effect of fragment size. To reduce the impacts of spatial nonindependence (autocorrelation) while maintaining the edge distance gradient, we rarefied CHM pixels systematically to grid with 10-m separation.

We test the significance of edge effects on average canopy height with a nonlinear regression using all 1-ha plots as samples; this analysis is not impacted by spatial nonindependence.

To assess potential effects and relationships, forest inventory variables (basal area, tree density, pioneers tree density, and AGB) were regressed on distance from the edge and structural attributes of the canopy from lidar (spatial heterogeneity and canopy openness fraction). Lidar-derived canopy structural attributes were related to long-term inventory variables with Pearson's correlation and univariate standard major axis regression, which assumes measurement error in predictor and response variables (Warton et al. 2006).

Results

Is canopy height influenced by proximity to forest edges and fragment size?

Considering mean canopy height among the six fragment and control forest plots, we found a significant relationships between distance to forest edge and canopy height, though with substantial unexplained variation (Appendix S1: Fig. S9; canopy height = 25.7 + 0.546 × (log(edge distance)); $P = 0.031$; $r^2 = 0.09$). We also observed that the plots <40 m from the edge had the lowest canopy heights relative to the interior mean (28.8 m), averaging 12% shorter. To better assess the form of this relationship, we fit Eq. 3 considering the full ALS canopy height survey data (Fig. 2). Coefficient values fitted for each fragment are specified in Fig. 3, where α (asymptote) is the height of vegetation in meters at the fragment interior and β (intercept) at the fragment edge, while γ is related to the change rate. All model coefficients were significant at $P < 0.001$ (though we note that P values may be impacted by spatial nonindependence not controlled by pixel rarefaction to a 10-m grid). Canopy height was lower at the edges and increased progressively until asymptoting at 19–39 m away from the edge. It is noteworthy to mention that pixels situated out of the forest fragment were excluded from the calculation, and thus the observed decrease in canopy height near fragment edges is an effect of forest fragmentation. Smaller

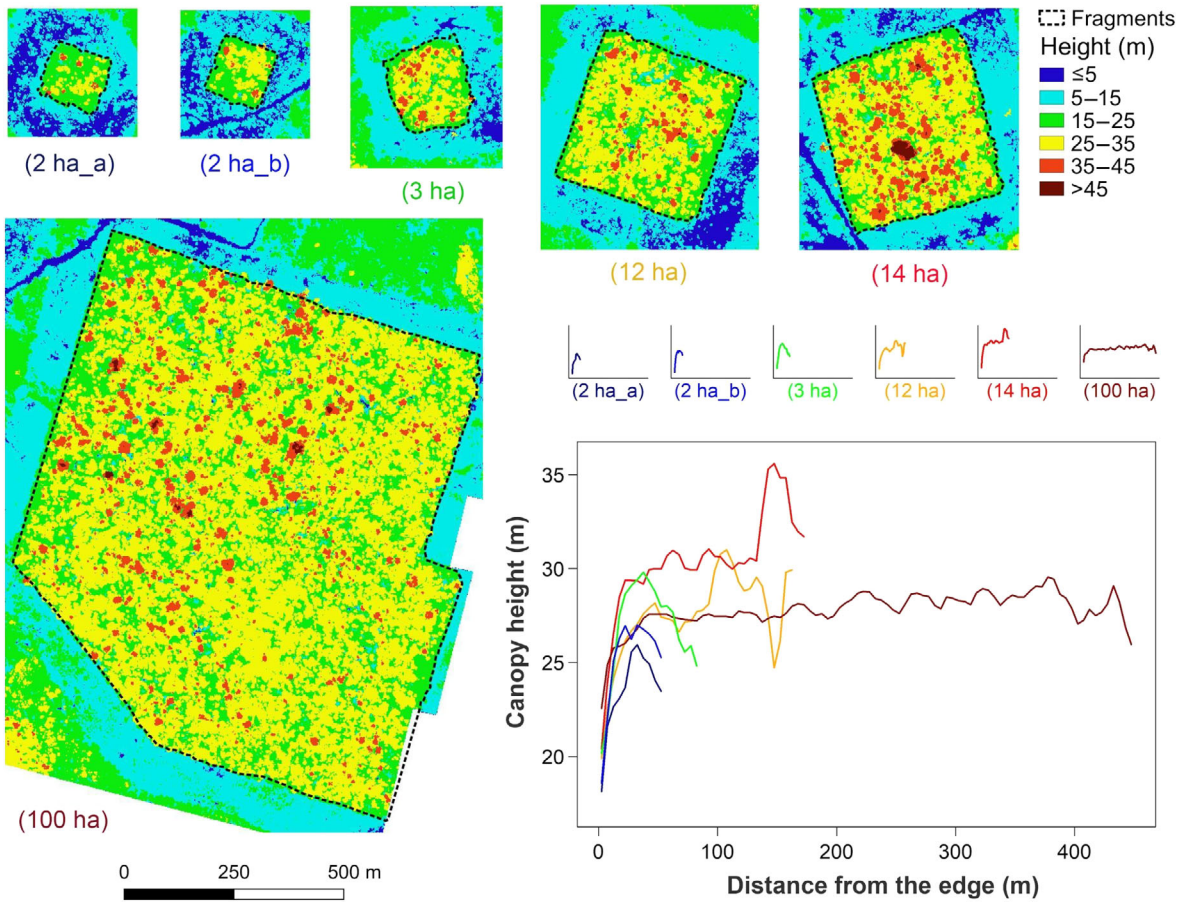

Fig. 2. Canopy height, obtained by airborne laser scanning, at different distances from the edge in six forest fragments in central Amazon, Brazil. The colored raster images are the canopy height model (CHM) of each fragment (2 × 2 m resolution). Lines in the graphs are the canopy height mean of all CHM cells in the respective distance class (5-m intervals). Canopy openness is shown by the blue pixels (CHM <15 m) within the fragments.

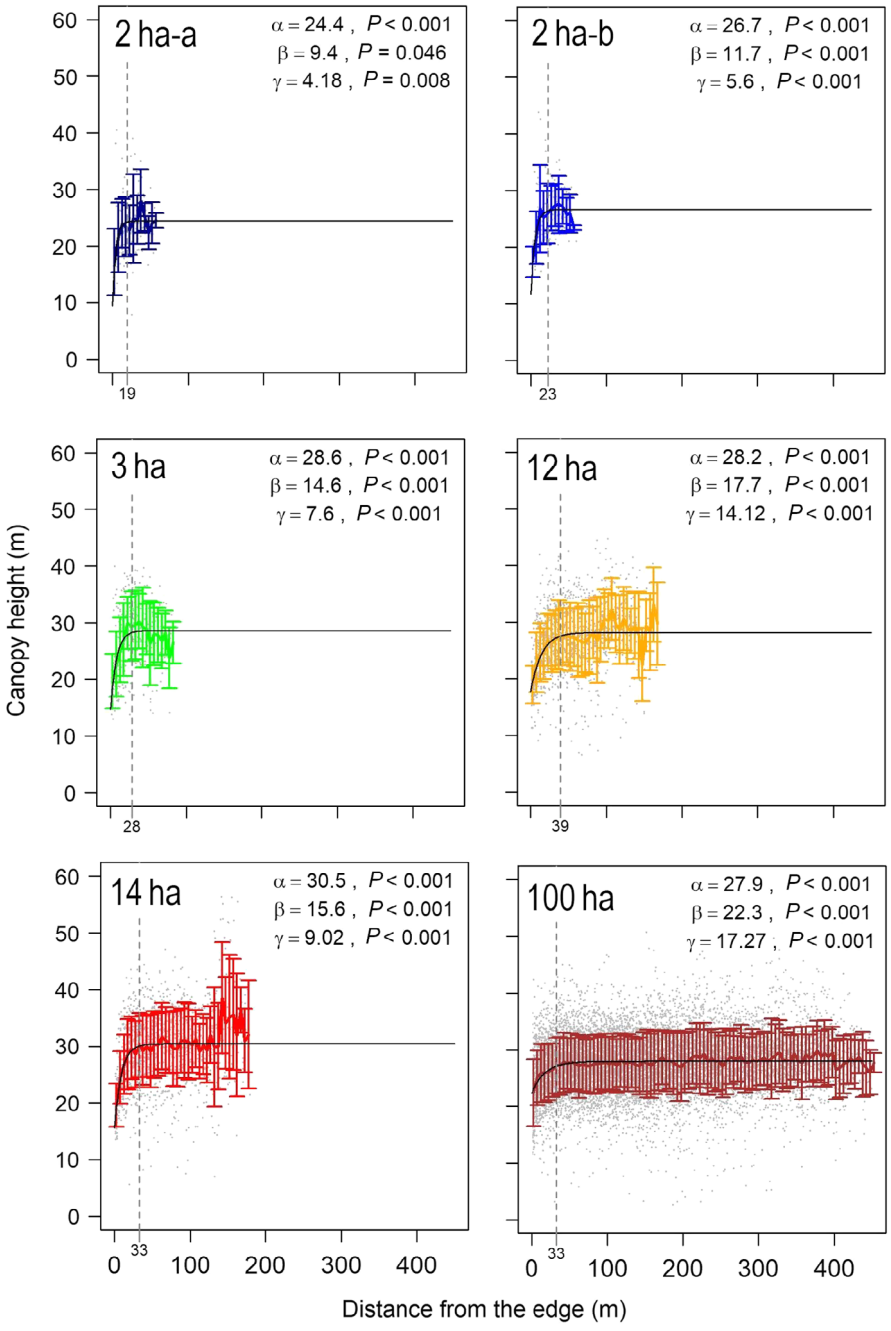

FIG. 3. Canopy height, obtained by airborne laser scanning, at different distances from edge in six forest fragments in central Amazon, Brazil. The gray dots are the height values of the canopy height model (resolution 2 × 2 m); the vertical dashed line indicates the distance where the rate of change in canopy height becomes <0.05 m; vertical bars are the standard deviation of heights in each distance class (5-m intervals). The parameter α is the asymptote of the model and represents the height at the fragment interior, β is the intercept of the model and represents the height of the canopy at the fragment edge, and γ determines the rate of change.

fragments (2 ha) appeared to have modestly, but consistently, lower canopy heights than larger fragments (maximum ~5-m difference at the interior; Fig. 4). The canopy height in the interior of the larger fragments was similar to the mean canopy height of the continuous forest plots (28.83 ± 1.25 m; mean ± SD; Appendix S1: Fig. S9).

As distance from the edge increases, the sample size (number of CHM pixels) inherently decreases. This may cause fragment interior estimates of mean canopy height to be more vulnerable to stochastic effects, and variation in mean height is elevated at greater distances from the edge (Figs. 2, 3). We also note that there were no clear

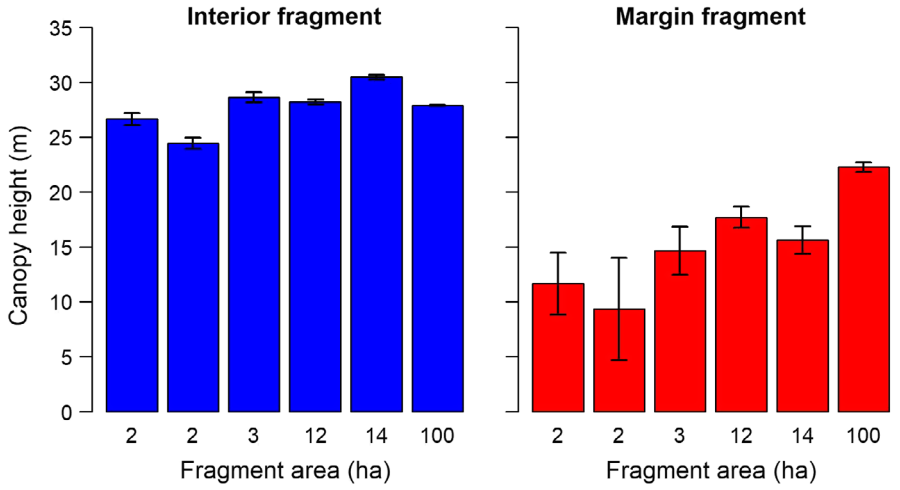

FIG. 4. Comparison of mean canopy heights, obtained with airborne laser scanner, at the interior (blue) and margin (e.g., within 40 m of edges; red) of forest fragments of different sizes, based on the fit parameters of Eq. 3 (*Methods*), among six forest fragments. Vertical bars express the 95% confidence intervals of the estimated coefficients.

relationships between canopy height and elevation, slope, or aspect in the BDFFP ALS survey data.

Are canopy openness and spatial heterogeneity influenced by proximity to forest edges and fragment size?

The canopy openness fraction ($P = 0.128$; Fig. 2 and Appendix S1: Fig. S10) was not related to distance from the edge. Canopy spatial heterogeneity increased with increasing distance from the edge in fragments of intermediate size (12 and 14 ha, $P < 0.001$), but showed no relationship with distance from the edge in the smallest and largest fragments (Fig. 5).

Are LAI and LAD profiles of different vertical strata influenced by proximity to forest edges?

The analysis of PCL data revealed, that the total LAI (LAI_{total}) was not related to distance from the edge ($P = 0.301$); however, LAD profiles did differ with distance from the edge of fragments (Fig. 6). By height classes, the LAI of the understory ($LAI_{1–5\ m}$) and upper ($LAI_{25–45\ m}$) strata increased with distance from the edge ($P = 0.025$ and $P < 0.001$, respectively), whereas LAI of the middle strata ($LAI_{5–15\ m}$ and $LAI_{15–25\ m}$) decreased as distance from the edge increased ($P < 0.001$ and $P = 0.012$; Fig. 6 and Appendix S1: Fig. S11).

Do negative impacts of edge proximity on basal area, AGB, and density of trees persist more than 20 yr after fragmentation?

In the first five years after fragmentation, basal area, AGB, and density of individuals (obtained from forest inventory data) were positively correlated to distance from the edge ($P < 0.001$ in all three cases; Fig. 7; Appendix S1: Figs. S12, S13, S14). Ten years after fragmentation, positive relationships remained for basal area and AGB ($P < 0.001$ for both), but not for tree density. Twenty-two years after fragmentation, however, basal area and AGB were no longer related to distance from the edge (Fig. 7; Appendix S1: Figs. S12 and S13), whereas tree density ($P = 0.005$; Fig. 7; Appendix S1: Fig. S14) and the proportion of pioneer trees ($P = 0.001$; Fig. 7; Appendix S1: Fig. S18) increased near edges.

Are canopy structure variables obtained by lidar able to reveal field metrics of fragmentation impacts?

We found significant correlations among variables obtained from lidar and forest inventories (Fig. 8). Canopy height was a significant predictor of AGB ($r^2 = 0.35$, $P < 0.001$). Lidar-derived canopy spatial heterogeneity (measured in 2008) was a significant predictor of change in basal area between the first and last inventories (1980–2008; $r^2 = 0.28$, $P < 0.001$), as well AGB ($r^2 = 0.35$, $P < 0.001$). Canopy height was also significantly correlated with (1) change in tree density from the pre-fragmentation state to 5 yr after fragmentation ($r^2 = 0.29$, $P < 0.001$, positive relationship) and (2) the proportion of pioneer individuals in the last inventory ($r^2 = 0.41$, $P < 0.001$, negative relationship). Both variables were correlated (negative relationship) with each other ($r = -0.59$, $P < 0.001$; Appendix S1: Table S1), and as described above, related to distance from edge. Canopy height, however, was a better predictor than distance from edge for the proportion of pioneer individuals, and both variables were significant in a multiple model ($r^2 = 0.50$, $P < 0.001$); the same was true for the change in tree density (multiple model: $r^2 = 0.46$, $P < 0.001$).

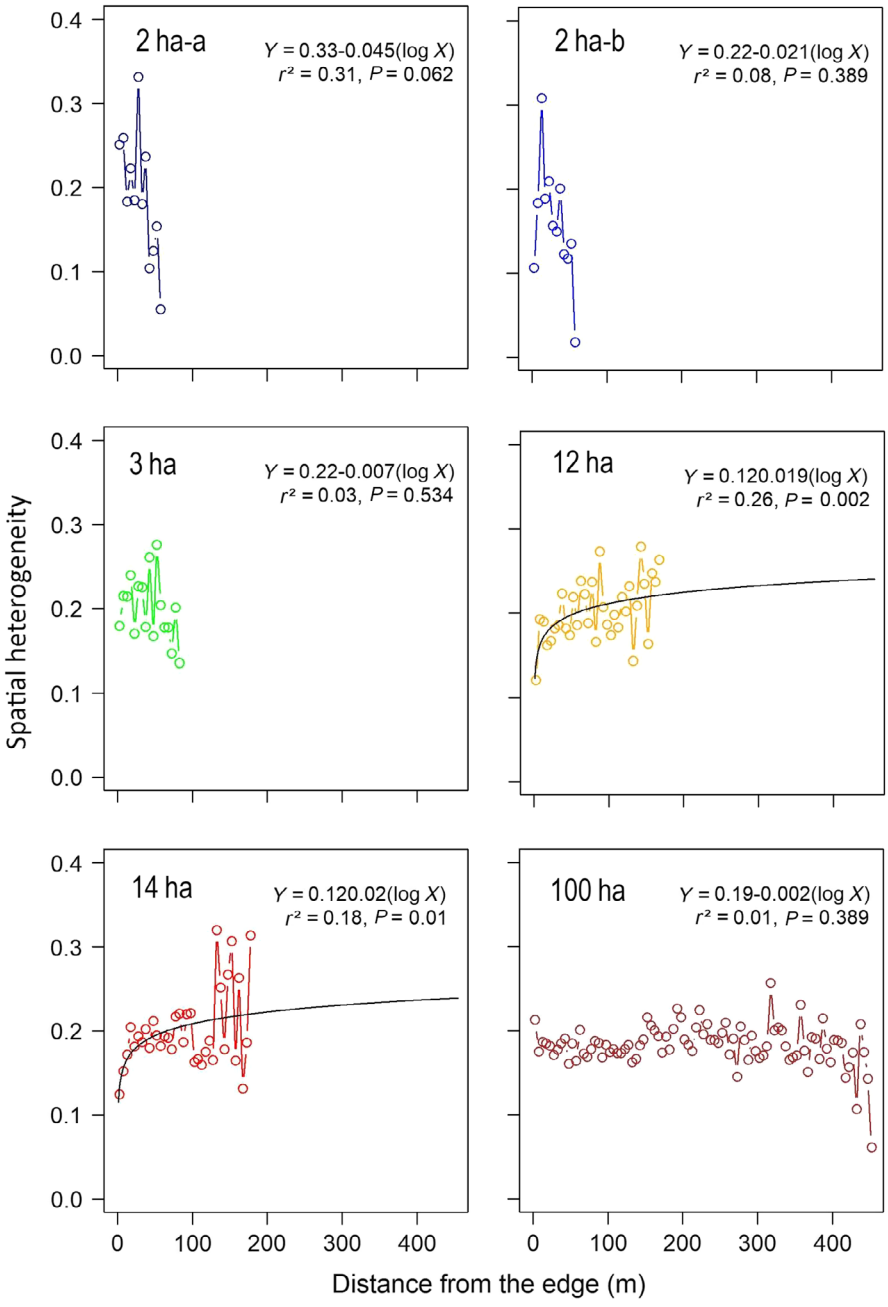

FIG. 5. Relationship between canopy spatial heterogeneity (coefficient of variation of canopy height), obtained with airborne laser scanner at 5-m intervals, and distance from the edge in six forest fragments. Points indicate canopy spatial heterogeneity for each 5-m interval while black solid lines show non-linear regression models.

DISCUSSION

Fragmentation effects on forest structure and dynamics changed with time, revealing both persistent and non-persistent impacts of forest fragmentation 20+ yr after fragment isolation. Overall, canopy height was persistently reduced near fragment edges and throughout small remnants, whereas AGB and basal area decreased in the first years after fragmentation, but recovered pre-fragmentation values after two decades. Near the edges, the leaf area index of the understory vegetation was lower, and leaf area index of the midstory higher, than in interiors. We attribute these results to the increased regeneration of pioneers following post-fragmentation mortality of large trees. Forest structure variables typically employed to assess the ecological impacts of

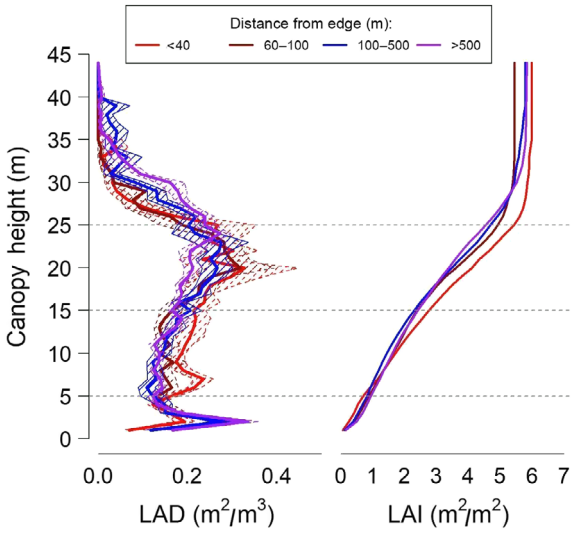

FIG. 6. Vertical profiles of leaf area density (LAD; left) and accumulated leaf area index (LAI; right) obtained with the portable profiling lidar (PCL). Dashed horizontal lines represent the four vertical strata analyzed. Line colors indicate distance-from-edge classes. Hashed regions surrounding LAD vertical profiles are the mean standard error.

fragmentation (AGB, basal area, density of individuals, and density of pioneer trees) were predictable from lidar-derived canopy surface variables, highlighting the potential of this technology for high precision, fast, and broader scale quantitative characterization of forest canopy structure changes and associated ecological impacts of fragmentation. In this section, we discuss in detail the integration of lidar technologies and forest inventory monitoring for the assessment of long term effect of forest fragmentation.

Canopy height

Canopy height was negatively influenced by proximity to forest edges and reduction of fragment size. Canopy height was lower at the edges of all six fragments surveyed, but especially in smaller fragments (2 ha), with persistent effects up to 41 m away from the edges. Canopy heights were reduced near edges most likely due to mortality of larger trees in the first few years after fragmentation, and the enhanced regeneration of shorter pioneer trees in the following years (Appendix S1: Figs. S17–19; Bierregaard et al. 1992, Ferreira and Laurance 1997, Laurance et al. 2006*a*, 2000). Two interrelated processes help to explain this phenomenon. First, the higher incidence of winds along edges is more harmful to large trees (Laurance et al. 2000, D'Angelo et al. 2004), which form gaps when they fall and stimulate the regeneration of pioneer species (Ferreira and Laurance 1997, Laurance et al. 2006*a*). In addition, soil desiccation, resulting from a higher incidence of dry and hot winds (Kapos 1989), and aggravated by higher incidence of radiation, favors ruderal trees and climber species that may keep forest edges in an arrested successional state (Ferreira and Laurance 1997, Laurance et al. 2006*a,b*).

Canopy gaps and spatial heterogeneity

Canopy openness and spatial heterogeneity (i.e., the coefficient of variation of canopy height) were not clearly influenced by proximity to forest edges. These two metrics related to forest dynamics and gaps (Stark et al. 2012, Hunter et al. 2015) offered mixed and inconclusive evidence of fragmentation impacts. Contrary to our expectations, canopy openness was not related to fragmentation. This may be explained by the regeneration of trees prior to lidar assessments. The most dynamic period occurred immediately after fragmentation (0–5 yr), when mortality of remnant trees increases substantially (Fig. 7; Laurance et al. 1998), which promoted the vigorous regeneration of pioneer trees (5–10 yr; Fig. 7) and lianas (Laurance et al. 2001). Furthermore, canopy openness was low throughout the study site, suggesting that other metrics may reveal canopy dynamics more effectively.

Canopy spatial heterogeneity did display potential impacts of fragmentation, increasing with distance from the forest edge, contrary to the hypothesized relationship; however, this was only observed in intermediate-sized fragments (12 and 14 ha). A potential alternative hypothesis predicting increasing heterogeneity with distance from the edge holds that low statured vegetation dominated by pioneers of a similar age (recruited following fragmentation) is more homogeneous. Interior forest, with the uneven age structure and a broader range of tree sizes typical of mature forest, on the other hand, may be expected to have more spatially heterogeneous canopy structure because of this broader demographic mosaic (Hardiman et al. 2011, Stark et al. 2012). In smaller fragments (~2 ha), fragmentation (and forest edges) may impact the canopy structure of the entire fragments; consistent with this there was little change in spatial heterogeneity between the edge and interior. However, canopy height of smaller fragments was higher in the interior than in the edges. In the larger fragment (100 ha), we hypothesize that there could be a size dependent buffer effect that reduces differences between spatial heterogeneity, and canopy height, in interior vs edge forest. Reduced negative impacts of microclimate alterations in the longer edges of the large fragment (Kapos 1989) could play a role if this is the case. Overall, canopy surface heterogeneity metrics did not respond clearly and consistently to edge effects, as was the case for canopy height.

Leaf area profiles

The vertical organization of the canopy, but not total LAI, changed with proximity to the edge. Previous studies (using a visual measurement approach) at the

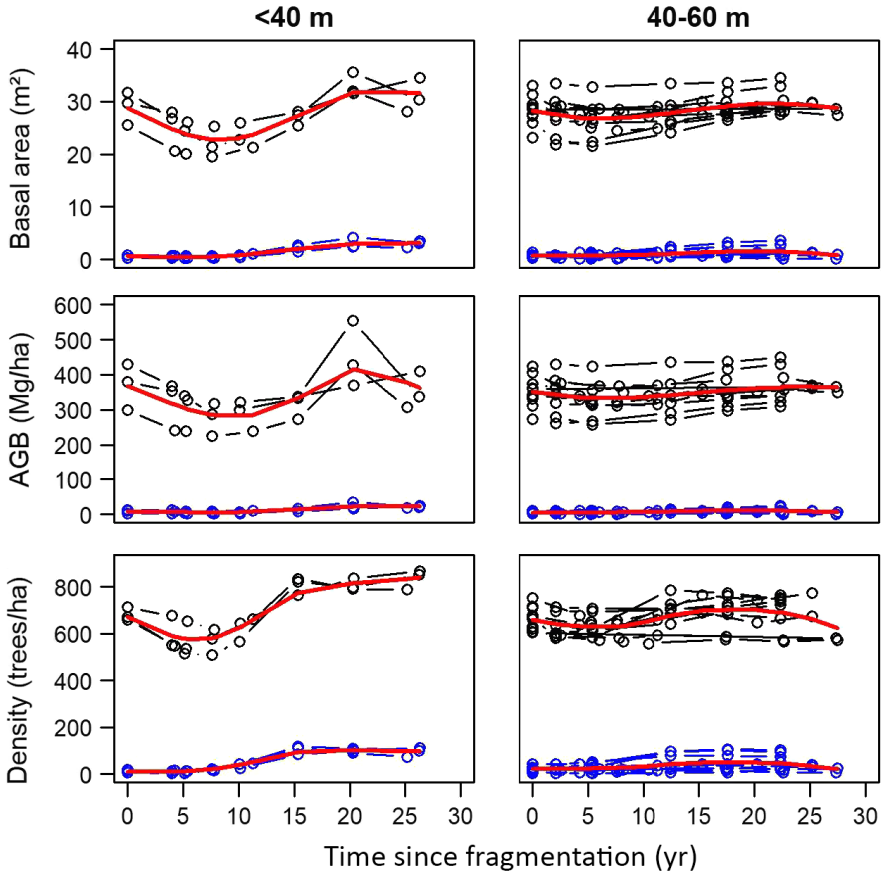

FIG. 7. Mean basal area, aboveground biomass (AGB) and density of trees over time (years after fragmentation), calculated from field inventory data, in two classes of distance from forest edges (<40 m, left graphs; 40–60 m, right graphs) of six forest fragments in central Amazon, Brazil. Black and blue colored circles and lines represent all species and pioneer species, respectively (i.e., pioneers are the lower groups); each blue or black line represents one plot. Red lines are means over all plots.

BDFFP project found that understory vegetation at fragment edges was denser than midstory vegetation (Malcolm 1994, Camargo and Kapos 1995). But we find the opposite pattern, with the highest vegetation density near edges occurring in the midstory. Even though these prior studies of leaf area profiles employed visual survey approaches, we expect comparisons using these simple canopy strata definitions to be accurate, and the pattern of change corresponds with expectations based on forest edge dynamics. Specifically, tree growth and regeneration at the edges in the ~20 yr since these first canopy structure studies most likely explain these contrasting leaf area profile observation; in this case, the relatively sparse midstory near forest edges in the 1990s, a direct consequence of the documented increases in tree mortality 5+ yr after fragmentation (Bierregaard et al. 1992, Ferreira and Laurance 1997), increased in LAD due to the abundant regeneration of pioneer trees (Fig. 7). The accumulation of vegetation in the middle stratum of the canopy may reduce light penetration and consequently limit the growth of new individuals in the understory. Thus, the reorganization of canopy structure near fragment edges appears to be the result of an ongoing regeneration process, rather than a new equilibrium; however, we acknowledge the need for caution comparing PCL results to plot surveys given the 6 yr time span between the plot inventories and more recent PCL lidar surveys.

Resilience of forest structure to fragmentation effects

Forest edges, rather than fragment interiors, displayed strong and dynamic responses to fragmentation in this and prior studies in the BDFFP. However, structural metrics obtained from forest inventories suggest the potential for a surprising resilience of forest patches to fragmentation effects. Even though edges exhibited losses in basal area, AGB, and tree density in the initial years after fragmentation, these variables were no longer different after 20+ yr, except tree density, which significantly increased near edges. The only consistent difference near edges among these factors was higher variation (Appendix S1: Fig. S12, S13, and S14). Although there was lower average plot AGB at the edges

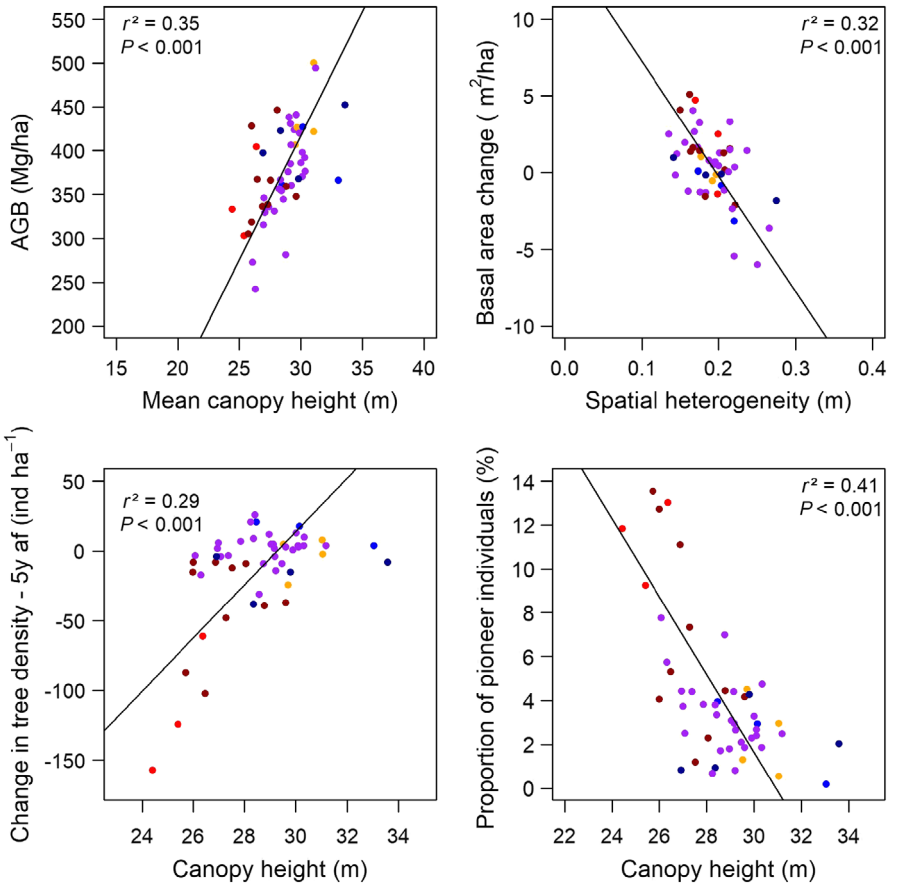

FIG. 8. Relationships between canopy structural variables measured by airborne laser scanner (*x*-axes) and field inventories (*y*-axes) in six forest fragments and adjacent continuous forest (>500 m). Each point represents a field plot, colored by median distance from the forest edge. Lines are standard major axis regressions.

10 years after fragmentation (Nascimento and Laurance 2006), AGB stocks appeared to recover on average after 5 more years (Fig. 7; Appendix S1: Figs. S13 and S16). Our results indicate that the immediate impacts of fragmentation on forest structure and function (specifically AGB) can partially recover in a few decades. As tree density and lidar-derived canopy structure metrics demonstrate, though, edge forest is ecologically differentiated relative to the pre-fragmentation state, even while AGB and basal area appear to have recovered substantially. Potentially explaining this apparent contradiction, higher densities of intermediate-sized, early successional individuals may have compensated for initial AGB and basal area losses caused by enhanced large remnant tree mortality. It is important to note that these fragments are part of a controlled experiment, where the edges have been protected from fire, tree harvest, and other anthropogenic impacts; biomass may be much less likely to recover if edges are exposed to these additional, potentially recurring, disturbances typically found in human-modified tropical landscapes (Barlow et al. 2016).

Canopy structure and forest field metrics

Canopy structure observations reveal critical elements of AGB stock and dynamics in forest fragments. Relationships between forest structure variables obtained from ALS and field inventories were highly significant, explaining 29–41% of variation (Fig. 8), comparable to similar studies of mature tropical forest sites in the region (Stark et al. 2012). Edge distance categories did not explain, or explained little (density change and pioneer density), additional variation in these relationships, and analyses included continuous (control) forest plots.

While both relationships were significant, the predictability of basal area change from canopy spatial heterogeneity was relatively higher than AGB change (r^2 = 0.28, using AGB). The relationships between forest structure (lidar) and function (AGB and AGB dynamics from inventory plots) within forest fragments did not differ from those observed in continuous forests. Fragmentation, in this case, impacts forest structure and forest function consistently, perhaps due to integral mechanisms linking these properties. The practical

implication of this finding is that lidar should prove robust in monitoring fragmentation impacts through time and over heterogeneous landscapes, expanding understanding developed through time consuming tree inventory monitoring.

The negative relationship between spatial heterogeneity and basal area and AGB change is likely a result of tree mortality and associated gap dynamics. In this case, tree loss is associated with loss of leaf area and probably the creation of gaps, which increase canopy heterogeneity. Gain from tree growth, on the other hand, may result from regeneration of pioneer trees in forest gaps, leading to lower heterogeneity. Tree wood density variation is potentially impacted by fragmentation due to increases in pioneer trees with low wood gravity (Appendix S1: Fig. S20; Laurance et al. 2006*b*); however, basal area and leaf area also increase with the regeneration of pioneer trees, regardless of the decline in the average wood density of the tree community.

Canopy height was also related to the proportion of pioneers, which have lighter wood and faster population dynamics, thus impacting carbon storage and turnover rates (Laurance et al. 1998, 2006*a*, Laurance 2002). Intriguingly, the change (in this case, "loss") in density of trees in the 5 yr that followed fragmentation was a predictor of canopy height at the time of the lidar survey some 20 yr later, though, seemingly, this relationship was only apparent near fragment edges. These relationships may be linked: initial tree loss (density decrease) led to high recruitment and regeneration of pioneer species (to densities higher than the initial state), which have lower stature than later successional species, and may have not achieved the pre-fragmentation height after 20 yr.

Conclusion

After more than 20 yr of isolation, the canopy structure and functional attributes (AGB and AGB dynamics) of forest fragments in the BDFFP displayed persistent and nonpersistent impacts, differentiating or not these forests from nearby contiguous areas, depending on the forest structure variable considered. While impacts on canopy height have been documented from forest inventory data in the BDFFP, these impacts have not previously been documented quantitatively with lidar, nor have the effects on canopy openness, canopy spatial heterogeneity, and LAI and LAD profiles been explored. Canopy height is negatively influenced by proximity to forest edges and small fragment size. Canopy openness and spatial heterogeneity are not clearly influenced by proximity to forest edges. The vertical organization of the canopy, but not total LAI, changes with proximity to edges. Considering just long-term BDFFP forest inventories, we also found that the previously reported initial negative effects of fragmentation on AGB stocks have been partially neutralized by ongoing forest regeneration near forest edges. In addition to AGB, other forest structure variables typically adopted to assess the ecological impacts of fragmentation (basal area, density of trees, and density of pioneer trees) may be estimated with lidar variables, though additional work is required to assess the generality and transferability of these relationships to other fragmented landscapes. Lidar technology offered novel insights into the ecological impacts of fragmentation on forest structure and function, helping reveal the persistence of canopy structural changes in the face of their potential partial recover in the post-fragmentation period, and enabling monitoring at much broader spatial scales than traditional methods. This will be particularly critical in the future as Amazon land use change continues under hotter and drier climatic conditions that have the potential to exacerbate the effects of forest fragmentation by promoting fire, water stress, and other disturbance factors.

Acknowledgments

We thank the whole Biological Dynamics Forest Fragments Project (BDFFP) team for the support and financing of the ground-lidar field collections through the Thomas Lovejoy Research Grant (2015), which was conducted also with support of the project "Como as florestas da Amazônia Central respondem às variações climáticas? Efeitos sobre dinâmica florestal e sinergia com a fragmentação florestal" (CNPq / Edital LBA). D. Almeida was supported by the São Paulo Research Foundation (#2016/05219-9 and #2018/21338-3), P. H. S. Brancalion by the National Council for Scientific and Technological Development (CNPq - grant #304817/2015-5), S.C. Stark by NSF (EF-1550686 and EF-1340604). R. Valbuena acknowledges support by the EU Horizon2020 Marie Sklodowska-Curie Action LORENZLIDAR (658180). This is study 758 of the BDFFP Technical Series.

Literature Cited

Almeida, D. R. A., S. C. Stark, G. Shao, J. Schietti, B. W. Nelson, C. A. Silva, E. B. Gorgens, R. Valbuena, D. A. Papa, and P. H. S. Brancalion. 2019. Optimizing the remote detection of tropical rainforest structure with airborne lidar: Leaf area profile sensitivity to pulse density and spatial sampling. Remote Sensing 11:92.

Barlow, J., G. D. Lennox, J. Ferreira, E. Berenguer, A. C. Lees, R. Mac. Nally, and T. A. Gardner. 2016. Anthropogenic disturbance in tropical forests can double biodiversity loss from deforestation. Nature. https://doi.org/10.1038/nature18326

Bierregaard, R. O., T. E. Lovejoy, V. Kapos, and R. W. Hutchings. 1992. The biological dynamics of tropical rainforest fragments. BioScience 42:859–866.

Brinck, K., R. Fischer, J. Groeneveld, S. Lehmann, M. Dantas De Paula, S. Pütz, and A. Huth. 2017. High resolution analysis of tropical forest fragmentation and its impact on the global carbon cycle. Nature Communications 8:14855.

Broadbent, E. N., G. P. Asner, M. Keller, D. E. Knapp, P. J. C. Oliveira, and J. N. Silva. 2008. Forest fragmentation and edge effects from deforestation and selective logging in the Brazilian Amazon. Biological Conservation 141:1745–1757.

Camargo, J. L. C., and V. Kapos. 1995. Complex edge effects on soil moisture and microclimate in central Amazonian forest. Journal of Tropical Ecology 11:205–221.

Chambers, J. Q., G. P. Asner, D. C. Morton, L. O. Anderson, S. S. Saatchi, F. D. B. Espírito-Santo, and C. Souza. 2007. Regional ecosystem structure and function: ecological

insights from remote sensing of tropical forests. Trends in Ecology and Evolution. https://doi.org/10.1016/j.tree.2007.05.001

Chaplin-Kramer, R., I. Ramler, R. Sharp, N. M. Haddad, J. S. Gerber, P. C. West, and H. King. 2015. Degradation in carbon stocks near tropical forest edges. Nature Communications 6:10158.

Chave, J., M. Réjou-Méchain, A. Búrquez, E. Chidumayo, M. S. Colgan, W. B. C. Delitti, and G. Vieilledent. 2014. Improved allometric models to estimate the aboveground biomass of tropical trees. Global Change Biology 20:3177–3190.

D'Angelo, S. A., A. C. S. Andrade, S. G. Laurance, W. F. Laurance, and R. C. G. Mesquita. 2004. Inferred causes of tree mortality in fragmented and intact Amazonian forests. Journal of Tropical Ecology 20:243–246.

de Almeida, D. R. A., B. W. Nelson, J. Schietti, E. B. Gorgens, A. F. Resende, S. C. Stark, and R. Valbuena. 2016. Contrasting fire damage and fire susceptibility between seasonally flooded forest and upland forest in the Central Amazon using portable profiling LiDAR. Remote Sensing of Environment 184:153–160.

De Oliveira, A. A., and S. A. Mori. 1999. A central Amazonian terra firme forest. I. High tree species richness on poor soils. Biodiversity and Conservation 8:1219–1244.

Didham, R. K., and J. H. Lawton. 1999. Edge structure determines the magnitude of changes in microclimate and vegetation structure in tropical forest fragments. Biotropica 31:17.

Ewers, R. M., R. K. Didham, L. Fahrig, G. Ferraz, A. Hector, R. D. Holt, and E. C. Turner. 2011. A large-scale forest fragmentation experiment: the Stability of Altered Forest Ecosystems Project. Philosophical Transactions of the Royal Society B 366:3292–3302.

Ferreira, L. V., and W. F. Laurance. 1997. Effects of forest fragmentation on mortality and damage of selected trees in central Amazonia. Conservation Biology 11:797–801.

Hardiman, B. S., G. Bohrer, C. M. Gough, C. S. Vogel, and P. S. Curtis. 2011. The role of canopy structural complexity in wood net primary production of a maturing northern deciduous forest. Ecology 92:1818–1827.

Hunter, M. O., M. Keller, D. Morton, B. Cook, M. Lefsky, M. Ducey, and R. Zang. 2015. Structural dynamics of tropical moist forest gaps. PLoS ONE. https://doi.org/10.1371/journal.pone.0132144

Kapos, V. 1989. Effects of isolation on the water status of forest patches in the Brazilian Amazon. Journal of Tropical Ecology 5:173–185.

Laurance, W. F. 2002. Hyperdynamism in fragmented habitats. Journal of Vegetation Science. https://doi.org/10.1111/j.1654-1103.2002.tb02086.x

Laurance, W. F., S. G. Laurance, L. V. Ferreira, J. M. Rankin-de Merona, C. Gascon, and T. E. Lovejoy. 1997. Biomass collapse in Amazonian forest fragments. Science 278:1117–1118.

Laurance, W. F., L. V. Ferreira, J. M. R. Merona, and S. G. Laurance. 1998. Rain forest fragmentation and the dynamics of Amazonian tree communities. Ecology 79:2032.

Laurance, W. F., P. Delamônica, S. G. Laurance, H. L. Vasconcelos, and T. E. Lovejoy. 2000. Rainforest fragmentation kills big trees. Nature 404:836–836.

Laurance, W. F., D. Pérez-Salicrup, P. Delamônica, P. M. Fearnside, S. D'Angelo, A. Jerozolinski, and T. E. Lovejoy. 2001. Rain forest fragmentation and the structure of Amazonian liana communities. Ecology 82:105–116.

Laurance, W. F., H. E. M. Nascimento, S. G. Laurance, A. C. Andrade, P. M. Fearnside, J. E. L. Ribeiro, and R. L. Capretz. 2006*a*. Rain forest fragmentation and the proliferation of successional trees. Ecology 87:469–482.

Laurance, W. F., H. E. M. Nascimento, S. G. Laurance, A. Andrade, J. P. Giraldo, T. E. Lovejoy, and S. D. Angelo. 2006*b*. Rapid decay of tree-community composition in Amazonian forest fragments. Proceedings of the National Academy of Sciences USA 103:19010–19014.

Laurance, W. F., J. L. C. Camargo, P. M. Fearnside, T. E. Lovejoy, G. B. Williamson, R. C. G. Mesquita, and S. G. W. Laurance. 2017. An Amazonian rainforest and its fragments as a laboratory of global change. Biological Reviews. https://doi.org/10.1111/brv.12343

Lefsky, M. A., W. B. Cohen, G. G. Parker, and D. J. Harding. 2002. Lidar remote sensing for ecosystem studies. BioScience 52:19–30.

Lovejoy, T. E., J. M. Rankin, R. O. Bierrgaard Jr, K. S. Brown Jr, L. H. Emmons, and M. E. Van der Voort. 1984. Ecosystem decay of Amazon forest remnants. Vol. 111, Pages 295–325. *in* Extinctions. University of Chicago Press, Chicago, Illinois, USA.

MacArthur, R. H., and H. S. Horn. 1969. Foliage profile by vertical measurements. Ecology 50:802–804.

Malcolm, J. R. 1994. Edge effects in central Amazonian forest fragments. Ecology 75:2438–2445.

McWilliam, A. L. C., J. M. Roberts, O. M. R. Cabral, M. V. B. R. Leitao, A. C. L. de Costa, G. T. Maitelli, and C. A. G. P. Zamparoni. 1993. Leaf area index and above-ground biomass of terra firme rain forest and adjacent clearings in Amazonia. Functional Ecology 7:310.

Nascimento, H. E. M., and W. F. Laurance. 2006. Efeitos de área e de borda sobre a estrutura florestal em fragmentos de floresta de terra-firme após 13-17 anos de isolamento. Acta Amazonica 36:183–192.

Nelson, B. W., R. Mesquita, J. L. G. Pereira, S. Garcia Aquino De Souza, G. Teixeira Batista, and L. Bovino Couto. 1999. Allometric regressions for improved estimate of secondary forest biomass in the central Amazon. Forest Ecology and Management. https://doi.org/10.1016/s0378-1127(98)00475-7

Nychka, D., R. Furrer, and S. Sain. 2015. fields: Tools for spatial data. National Center for Atmospheric Research. https://cran.r-project.org/web/packages/fields/fields.pdf

Parker, G. G., D. J. Harding, and M. L. Berger. 2004. A portable LIDAR system for rapid determination of forest canopy structure. Journal of Applied Ecology 41:755–767.

QGIS Development Team. 2015. QGIS Geographic Information System. Open Source Geospatial Foundation Project. https://www.qgis.org/

R Core Team. 2017. R: A language and environment for statistical computing. R Foundation for Statistical Computing, Vienna, Austria.

Runkle, J. R. 1982. Patterns of disturbance in some old-growth mesic forests of eastern North America. Ecology. https://doi.org/10.2307/1938878

Simonson, W. D., H. D. Allen, and D. A. Coomes. 2014. Applications of airborne lidar for the assessment of animal species diversity. Methods in Ecology and Evolution. https://doi.org/10.1111/2041-210x.12219

Stark, S. C., V. Leitold, J. L. Wu, M. O. Hunter, C. V. de Castilho, F. R. C. Costa, and S. R. Saleska. 2012. Amazon forest carbon dynamics predicted by profiles of canopy leaf area and light environment. Ecology Letters 15:1406–1414.

Tang, H., and R. Dubayah. 2017. Light-driven growth in Amazon evergreen forests explained by seasonal variations of vertical canopy structure. Proceedings of the National Academy of Sciences USA 114:2640–2644.

Valbuena, R., M. Maltamo, L. Mehtätalo, and P. Packalen. 2017. Key structural features of Boreal forests may be detected directly using L-moments from airborne lidar data. Remote Sensing of Environment 194:437–446.

van Leeuwen, M., and M. Nieuwenhuis. 2010. Retrieval of forest structural parameters using LiDAR remote sensing. European Journal of Forest Research. https://doi.org/10.1007/s10342-010-0381-4

Warton, D. I., I. J. Wright, D. S. Falster, and M. Westoby. 2006. Bivariate line-fitting methods for allometry. Biological Reviews of the Cambridge Philosophical Society. https://doi.org/10.1017/s1464793106007007

Zanne, A. E., G. Lopez-Gonzalez, D. A. A. Coomes, J. Ilic, S. Jansen, S. L. S. L. Lewis, and J. Chave. 2009. Global wood density database. Dryad 235:33.

Supporting Information

Additional supporting information may be found online at: http://onlinelibrary.wiley.com/doi/10.1002/eap.1952/full

Data Availability

Data are available from Zenodo: https://doi.org/10.5281/zenodo.3241782